Finite element lower bound "yield line" analysis of isotropic slabs using rotation-free elements

A. Salam Al-Sabah*

Research Scientist
University College Dublin

Holger Falter

Professor
Coburg University of Applied Sciences
Former Lecturer, University College Dublin

* Corresponding author. Tel.: +353 87 935 6826; fax: +353 668 3169. E-mail address: abd.al-sabah@ucdconnect.ie

ABSTRACT

A new lower bound finite element method for slab analysis is presented as a practical substitute to full, non-linear, finite element methods that require expert knowledge and long running times. The method provides a general, safe and efficient lower bound solution for the analysis of reinforced concrete slabs up to failure. As it is finite element based, the method is more general than the yield line and strip methods currently in use. Furthermore, its lower bound nature makes it safer than the yield line method. The method uses a rotation-free, plate finite element modified to allow plastic "yield lines" to pass through at any direction. Yield lines are generated at the principal moment directions when the plastic moment capacity is attained. The material is assumed to be elastic perfectly-plastic. Following the general spirit of yield line analysis, the effects of a yield line are projected to the sides of the triangular element and then used to calculate the bending curvatures. The method's efficiency is achieved by using rotation-free plate elements with a single degree of freedom per node and by the incremental solution that does not require iterations. The method's accuracy and convergence are assessed by comparing standard cases with known results. In all cases, results were close to the theoretical values with difference of less than 1%. It is also used to solve a practical sized flat slab problem in order to demonstrate the method's efficiency, convergence, and speed.

1. Introduction

Yield line analysis is a powerful method to predict the collapse load of reinforced concrete slabs. The term "yield line" was first introduced by Ingerslev in 1921 [1]. Later, Johansen [2] proposed a systematic analysis with a geometric interpretation of the concept. Mainly through the work of Johansen [3], Nielsen [4] and Jones and Wood [5] was the yield line analysis of reinforced concrete slabs introduced into the wider structural engineering community. Today, yield line analysis has been applied to a wide range of applications from finding the collapse load of reinforced concrete slabs to that of steel connections [6, 7], steel base plates [8] and walls [9, 10].

The yield line analysis starts from an assumed collapse mechanism, the yield collapse pattern. By considering all kinematically admissible collapse mechanisms, the smallest ultimate load is taken as the final solution. This can be carried out by the virtual work method or the equilibrium method. The methods are related to each other [5], and the result is an upper bound solution to the collapse load.

To guarantee the kinematic admissibility of an assumed yield pattern, certain conditions related to the shape, position and arrangement of yield lines must be satisfied. The bending moment along the yield lines is assumed to be constant and equal to the plastic moment capacity of the slab. To simplify the analysis, the slab's elastic deformations are assumed to be negligible compared to the plastic deformations. This leads to a rigid-perfectly plastic behaviour.

During the early days of the yield line method, it was considered to be the most advanced analysis technique for reinforced concrete slabs. It attracted considerable interest from engineers and researcher due to its intuitive simplicity, accuracy and ability to analyse slabs of arbitrary geometry, reinforcement, support conditions and loading [3, 5]. However, two main issues were later identified as potential drawbacks. The first was the fact that it is an upper bound analysis as the analysis starts from assumed collapse mechanisms (the yield collapse pattern). In nearly all cases, this limits the

correct collapse load to only one yield pattern, while all other patterns result in higher, hence unsafe, collapse loads. Even after examining what appear to be all kinematically admissible yield patterns, there will remain an element of doubt about the existence of yet another pattern that is the true lower bound. Many such cases were reported. An overestimation of the collapse loads by up to 50% is possible [11], which undoubtedly affected the reliability perception of the yield line analysis.

The second issue was that for practical shaped slabs and boundary conditions, the correct yield patterns can be quite complicated. This task is far from trivial due to the excessive time required to identify and investigate all possible yield patterns to obtain the safe collapse load. As a result, hand-based, yield line analysis was limited to the simple slab cases only. With the widespread adoption of computers in structural analysis and developments in matrix structural analysis, attempts to resolve the above issues focused on automated, computer-based yield line analysis. In pioneering research Munro and Da Fonseca in 1978 [12] used triangular finite elements in a fixed mesh arrangement to find yield patterns. This avoided having to select an initial yield pattern. Equilibrium or compatibility conditions, yield constraints and an optimization function were established and solved using linear programming to find the critical yield pattern, but assumed that yield lines can only develop along element edges. Two single panel examples and one multi-panel example were solved with reasonable accuracy.

Subsequently, continuous attempts were made to resolve the inability to guarantee identification of the critical yield pattern. The finite element mesh had a fixed, initial pattern based on the expected yield pattern. If the correct yield pattern was definable by the mesh arrangement, then the results should be identical to correct results, otherwise only approximate results would be obtained.

Dickens and Jones in 1988 [13] used a manually assisted computer method to progressively adjust an assumed trial yield pattern manually. Single panel examples were solved by the proposed method.

In 1994 Johnson [14] departed from the previous trend of researches by not relying on an initial yield pattern. Instead, a rigid-plastic yield-line analysis of isotropic slabs was conducted. Sequential linear programming was then used to successively correct the yield pattern. However the technique was inappropriate for fine finite element meshes due to difficulties in ensuring the straightness of yield lines and the correctness of the mesh topology. In such cases, the analysis was split into two stages. First, a linear finite element analysis was conducted using triangular elements. Then yield pattern was based on the results. A less refined mesh with element boundaries lying close to the expected yield lines was then constructed. Sequential linear programming was then applied to this mesh. It was assumed that yield lines can only develop along the element boundaries. The method was determined to be most appropriate for rectilinear slabs in order to avoid complex yield patterns.

Soon after Gohnert and Kemp [16] presented a new, four-noded finite element called the yield line element. The proposed method was mixed in the sense that moments and out-of-plane deflections were chosen as the unknowns. The solution matrix was developed from flexibility and equilibrium equations. Flexibility equations, expressing the relationship between the rotations and nodal moments, assumed as a partial quadratic moment field and equated to obtain inter-element compatibility. Gohnert in 2000 [17] presented the results of using this element in a yield line analysis. The moments were assumed to be linear–elastic, until the plastic moment was reached. At this point, the moment capacity of the member was assumed to be constant. Ten test cases with a variety of boundary, loading, and reinforcement conditions were presented. In the majority of cases, the solution was within 10% of the yield line result.

Middleton [18] in 1997 suggested a method through which the user can select patterns from a predefined library of failure mechanisms to assess bridge decks. The method was basically an upper bound solution based on yield line analysis. A computer program, COBRAS [19], was specially developed to carry out the required geometrical relationships for the failure mechanisms. Currently, COBRAS has 27 built-in failure mechanisms. It was used for assessing the ultimate load carrying capacity of over twenty bridges which were found to be unsatisfactory in carrying the full 40 tonne

requirement based on an elastic analysis. Of these bridges, 70% were found to pass the requirements when assessed using COBRAS.

Thavalingam et al. in 1998 [20] proposed a semi-automatic, yield line analysis of slabs starting from an approach similar to that by Munro and Da Fonseca [12]. However, the initial trial yield pattern was expressed by node positions treated as variables. The load factor was expressed as a function of node positions. By treating the load factor as the objective function subject to the previously described constrains, a non-linear optimization was applied to minimize the objective function by revising the initial yield pattern. An elaborate optimization procedure using line search method in addition to the conjugate gradient method was adopted. Three examples were solved. One was compared to the theoretical solution where a difference of less than 0.4% was reported. This research provided a method to automatically adjust a yield pattern. However, it was not completely user independent, as optimization started from a general, user-defined yield pattern.

Kwan [21] in 2004, proposed a new method to automatically define the initial yield pattern and then to adjust it to produce the minimum load factor. The method was based on defining the yield lines based on the dip (rotation) and strike (orientation of axis of rotation) angles. As such, the resulting yield pattern was kinamatically admissible. The load factor, as a function of the dip and strike angles, was then obtained using virtual work. A successive parabolic minimisation technique was then used to minimize the load factor, which was considered to be the objective function. Eight examples were solved. Good accuracy was reported with a difference of less than 1% when compared with theoretical or previously reported results by other researchers. The main limits were the applicability to only convex polygonal slabs and that the method was applicable only when the whole slab area took part in the collapse mechanism.

Wüst and Wagner [22] in 2008 presented a new method to systematically find all possible yield patterns of arbitrary polygonal plate. Both convex and concave cases were considered. Each individual pattern was then refined through an optimization procedure to obtain the minimum load factor, which was treated as the objective function. The algorithm used to find all possible yield patterns was based on the application of Catalan numbers and binary trees. Each resulting pattern was then triangulated with elements similar to those used by Munro and Da Fonseca [12]. The optimization part was conducted with either a direct search method or a conjugate gradient method. The first produced more reliable results independent of the initial values with a penalty of more time required than the conjugate gradient method. Three examples of single panel polygonal slabs of different complexities were solved. Results were compared with non-linear finite element results. The reported difference was 0.3% for a simple case increasing to 3%-7% for the more complex examples. This method was the first to automatically generate and consider all possible yield patterns in both concave and convex polygonal panels.

To date the methods have had only limited applicability to slabs of the geometry, load and boundary conditions encountered in usual structural design work. The main drawbacks are:

- The combination of finite element and optimization is able to solve small sized examples. However, the objective function derivatives are not continuous. Yield lines are usually located at points of derivative discontinuity. This results in difficulties in solution optimization [15, 20]. Even more difficulties are expected when attempting to solve large problems with hundreds of optimization variables rather than few tens.
- The optimization part is required to resolve the limitation that yield lines can only develop on the sides of the triangular elements.

An alternative to the upper bound yield line analysis is to use the Hillerborg lower bound strip method [23], which assumes that the total load is distributed between two sets of strips assumed to be orthogonal. The load distribution between the sets is arbitrary and will usually result in a safe design, if design code requirements related to ductility are satisfied [24].

Only limited efforts have been made to automate the Strip Method. In 1998, O'Dwyer and O'Brien [25] divided a slab into a grid of rectangular elements with a node at the centre of each element. The equilibrium of each node in the vertical direction was calculated numerically using the second difference. The method used a two-stage optimization procedure. It distinguished between analysis and design cases. The first optimization stage aimed to find the maximum collapse load and the minimum reinforcement in the analysis and design cases respectively. These quantities were considered to be the objective function in the linear programming used at this stage. The constraints were used to impose equilibrium and moment limits of the reinforced concrete slab. In the second stage, quadratic optimization was used to minimise the sum of squares of the differences between the first stage moment results and the corresponding elastic values. The method was used to solve a square slab free on one side and simply supported on the other three sides. The collapse load was within 2% of the yield analysis results.

More recently, Burgoyne and Smith [24] presented an automated lower bound method for the automatic assessment of existing reinforced concrete slabs. Optimization was used to find the highest lower bound load that did not violate the slab moment capacity. The equilibrium equation was written in a form where the internal load vector was expressed as the sum of two vectors. The first was related to an equilibrium state of the system, while the second was a set of self-stress vectors multiplied by a column vector of unknown coefficients. The method was used to solve a simply supported square slab and a short single span slab with concentrated loads. Convergence was reported to be slow. In addition, the result was 33% lower than the lowest upper bound. Similar result, 41% less than the benchmark value, was reported when a fixed square slab under uniform load was solved. The strip method, which usually ignores the torsional term in the equilibrium equation, was unable to effectively solve problems where the slab failure yield pattern was not parallel to the strips. The addition of two more sets of strips running at 45 degrees relative to the first improved the results with a predicted collapse load being 3.9% less than the benchmark value.

The most obvious alternative to both the yield line and strip methods is the non-linear finite element method. No initial prediction of yield pattern is required as yielding is automatically updated at each load increment. This analysis also allows the use of more realistic material properties, the ability to trace the slab behaviour at different loading stages and the generation of more information about the slab such as deflections and reactions. Powerful commercial software is available to analyse slabs up to collapse (ANSYS, SOFiSTiK, LS-DYNA and others). However, such a task is still not straightforward. It requires detailed definition of material properties, solution techniques, and convergence criteria limits. When applied to reinforced concrete slabs, the large degree of non-linearity due to concrete cracking can cause numerical instability that might cause the solution to diverge or even crash. In addition, the time required to solve practical sized problems is substantial, even with the use of desk computers having the latest multi-core processors. This is mainly due to the technique used in solving the non-linear stiffness equation. The solution is usually an incremental-iterative one. Loads are applied in increments followed by iterations to reduce the residue or unbalanced forces generated by the problem's non-linearity. In the case of non-linear analysis of reinforced concrete, concrete cracking can cause sudden release of strain energy. To stabilize the solution, smaller load increments and more iterations are used. The processing time penalty can be significant, particularly in large problems.

As a result, using non-linear finite element software requires deep knowledge of finite elements, non-linear analysis, and material constitutive relations, as well as sufficient time to refine the model parameters and solution. All these factors make this type of analysis beyond the reach of many design offices and/or project budgets.

2. Methodology

The aim of this research is to provide a method to analyse practical sized isotropic reinforced concrete slabs up to collapse without the difficulties usual encountered while using current non-linear finite element analysis solutions or the limitations of the yield line and strip methods.

2.1. Existing Rotation-free triangular plate element

The element by Munro and Da Fonseca [12] is triangular with an out-of-plane displacement degree of freedom at each node, Fig. 1. The element is assumed to be a rigid plate, and an angle of rotation of each edge (θ^e) of the element (e) constant along each side. The kinematic equation relating the rotation of each edge of a triangular element to nodal displacement (w) can be expressed as Eq. (1):

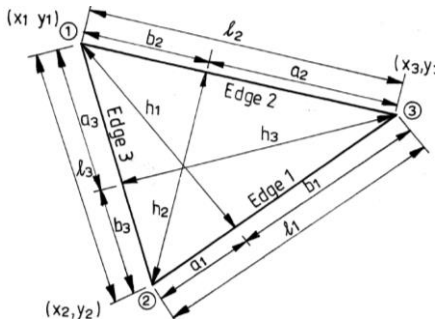

Fig. 1. Element used by Munro and Da Fonseca [12]

$$\begin{bmatrix} \theta_1^e \\ \theta_2^e \\ \theta_3^e \end{bmatrix} = \begin{bmatrix} -\frac{1}{h_1} & \frac{b_1}{l_1 h_1} & \frac{a_1}{l_1 h_1} \\ \frac{a_1}{l_2 h_2} & -\frac{1}{h_2} & \frac{b_2}{l_2 h_2} \\ \frac{b_3}{l_3 h_3} & \frac{a_3}{l_3 h_3} & -\frac{1}{h_3} \end{bmatrix} \begin{bmatrix} w_1 \\ w_2 \\ w_3 \end{bmatrix} \quad (1)$$

Arguably Eq. (1) is only a geometric relation between nodal displacements and the resulting edge rotations for a rigid element and not a representation of element stiffness. However, the main underlying concepts are:

a- The element is considered to be rigid
b- As a result of (a) above, all edge rotations can be related to out-of-plane nodal displacements
c- As a result of (a) and (b) above, there is no need to have rotational degrees of freedom

Since the time of publishing the work of Munro and Da Fonseca in 1978, many new developments in the finite element method have occured. New element types were developed. Among them was a plate element family called the "rotation-free" (RF) plate element. Their origins can be traced back to Nay and Utku [26], Hampshire et al [27] and Phaal and Calladine [28]. Most of these and related research were influenced by an element called "Morley Triangle" [29].

The main advantages of using RF plate elements are:

- Fewer degrees of freedom per node. Instead of the usual three degrees of freedom per node in a plate element (one vertical displacement and two rotationl), only one degree of freedom occurs.
- Element formulation is simpler, hence requiring less computation time.

On the other hand, RF elements have some disadvantages:

- Element has constant curvature. Results are less accurate than these obtained from more complicated elements with varying curvature. More constant curvature elements are required to achieve the same accuracy of the more complicated elements.
- Element stiffness matrix is related to the surrounding elements; hence global stiffness matrix bandwidth will increase.
- RF element formulation does not allow easy incorporation with existing finite element codes.
- RF elements are usually sensitive to mesh distortion.
- Rotational boundary conditions are not straightforward to define.

On the balance, it is still computationally advantageous to use RF plate elements in applications that have known difficulties when usual finite elements with rotational degrees of freedom are used.

The concepts behind deriving the stiffness matrix of triangular RF plate elements are the following:

- The element has constant curvature, hence constant moment.
- Curvature can be related to the out-of-plane nodal displacement of the element and three other out-of-plane nodal displacements from the three surrounding patch of elements.
- Usually a virtual work principle is used to derive the stiffness matrix.

The main difference between RF plate elements is the use of different approaches to relate the curvature to the element out-of-plane displacement and those of the surrounding elements, Fig. 2.

Fig. 2. Rotation-free element (e) surrounded by three elements

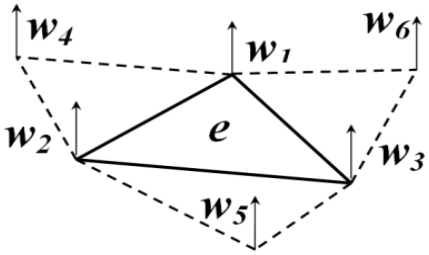

Sabourin and Brunet [30] related the rigid body rotation of the main element (e) sides to the out-of-plane nodal displacements, similar to the approach by Munro and Fonseca [12]. The rigid body rotations of the three elements surrounding element (e) on their common sides with element (e) were found similarly. The rigid body rotations were then related to the curvature on the three sides of the main triangle (e), which in turn was used to find the element constant curvature by superposition. Phaal and Calladine [28] used a complete quadratic polynomial in two dimensions to interpolate between the six out-of-plane nodal displacements. Constant curvature was obtained as derivatives of the displacement polynomial. This was achieved at the price of more computations. Onãte and Cervera [31] integrated the curvature over the element area and obtained an expression for the average constant curvatures of the element. The integration was conducted in parts. The resulting curvature was expressed as a summation over the three element sides of the displacement derivatives normal to each side.

Among the different alternatives to curvature calculations, the one that can be implemented in a manner closest to the spirit of the yield line analysis is the Sabourin and Brunet approach [30]. The main aspects of the element are presented below.

2.1.1. Existing RF element "S3"

The "S3" element derived by Sabourin and Brunet [30] has its roots in the Morley Triangle [29]. The out-of-plane deflection (w) within the triangle comes from a linear, rigid-body deflection (w^r) due to the nodal translations w_1, w_2, w_3 and from the quadratic "bending" deflection (w^b), Figs. 3 and 4.

The rotation angles (θ_i) on each side of the triangle (i) are the displacement derivatives in the direction normal to the sides. They consist of a rigid part (θ_i^r) and a bending rotation part (θ_i^b):

$$\begin{Bmatrix}\theta_1\\ \theta_2\\ \theta_3\end{Bmatrix} = \begin{Bmatrix}\theta_1^r\\ \theta_2^r\\ \theta_3^r\end{Bmatrix} + \begin{Bmatrix}\theta_1^b\\ \theta_2^b\\ \theta_3^b\end{Bmatrix}, \text{ or in a compact form as: } \{\theta\} = \{\theta^r\} + \{\theta^b\} \quad (3)$$

The curvature of each side (i) of the main triangle $\{\kappa_i\}$ can be calculated from the bending angles as follows:

$$\begin{Bmatrix}\kappa_1\\ \kappa_2\\ \kappa_3\end{Bmatrix} = [H_e]\begin{Bmatrix}\theta_1^b\\ \theta_2^b\\ \theta_3^b\end{Bmatrix}$$, or in a compact form as: $\{\kappa\} = [H_e]\{\theta^b\}$ (4)

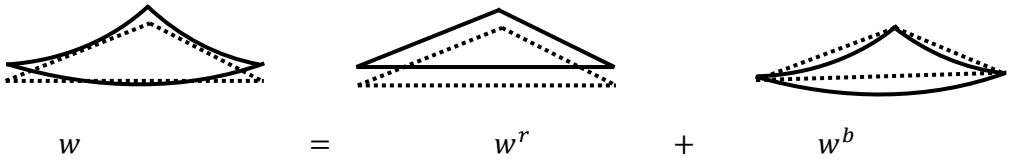

Fig. 3. Out-of-plane element deformation

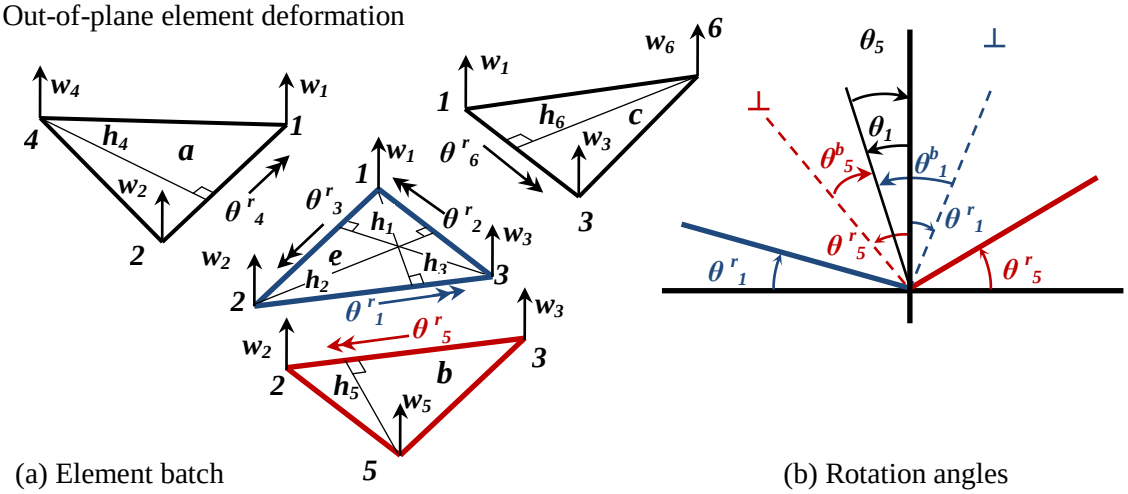

(a) Element batch (b) Rotation angles

Fig. 4. Relation between main components (a) and relation between interface angles (b)

By applying superposition, the curvature of the element can be calculated from the curvatures of the three sides of the triangular element.

Using the above relations, the constant curvature of the main triangle can be expressed as:

$$\{\boldsymbol{K}\} = \begin{Bmatrix}\kappa_{xx}\\ \kappa_{yy}\\ 2\kappa_{xy}\end{Bmatrix} = [R_e]\,\{\kappa\}$$ (5)

The main remaining part of the element derivation is the relation between bending and rigid rotation angles. These details will be described later as they are modified to allow for internal element yield lines, essential to the current work.

Resulting from these calculations is a relationship between the bending and rigid rotation angles:

$\{\theta^b\} = [H_v]\{\theta^r\}$ (6)

While in general terms, rigid deformations of a single element produces zero strain energy, the combined deformation of the four element assembly can produce strain energy related to the generated curvatures.

The relationship between the rigid rotation angles(θ^r) and the out-of-plane displacements (w) can be written as:

$\{\theta^r\} = [C]\{w\}$ (7)

Further details on $[H_e]$, $[R_e]$, $[H_v]$ and $[C]$ can be found in Ref. [32].

Combining the above equations, the following relationship can be written:

$$\{\boldsymbol{K}\} = [R_e]\,\{\kappa\} = [R_e]\,[H_e]\{\theta^b\} = [R_e]\,[H_e][H_v]\{\theta^r\} = [R_e]\,[H_e][H_v][C]\{w\} \quad (8)$$

Or in a compact form as:

$$\{\boldsymbol{K}\} = [\mathrm{B}]\{\mathrm{w}\} \quad (9)$$

Using virtual work principle, the stiffness matrix can be found as:

$$[K_e] = \int [B]^T [D][B] dv \quad (10)$$

Examples of the performance of element S3 under different load conditions, including twisting moment, were presented by Sabourin and Brunet [30]. Comparisons were made with both analytical solutions and these obtained using other type of elements. The results indicated that the element performance was reasonably accurate.

2.2. Development of current method

2.2.1. Discontinuity passing through element

The main issue identified in previous attempts of automated yield line analysis is the limitation that the yield line must be located on the boundary between two elements. This is difficult to predict without an initial analysis. So far, the methods used to resolve this issue can be categorised as follows:

- Running an initial linear finite element analysis using a fine mesh to identify potential yield pattern. Then using this pattern in a yield line analysis with an optimization algorithm to find the pattern that produces the least load factor [14].
- Based on the geometry of the slab, all the possible yield patterns are automatically found. Each pattern is investigated using an optimization algorithm to locate the minimum load factor for each pattern. The least value of the collection of minimum load factors resulting from the previous step is the load factor [22].

Both of these approaches have their limitations. The first approach requires a two-stage solution with manual intervention in between to select the most probable yield pattern. However, there is no guarantee that the chosen yield pattern is the correct one. This is because the solution is based on an initial elastic analysis. The second approach is more reliable in producing a correct yield pattern or one that is close to it. However, the penalty is that considerable time is required to investigate all possible yield patterns.

The alternative to automated yield line analysis is the use non-linear finite element analysis. No initial prediction of yield pattern is required. However the analysis is more involved as discussed earlier in section 1.

The possible solutions to a discontinuity passing through a finite element are as follows:

- Re-meshing the problem to create an element interface at the discontinuity. This is an expensive approach as the problem size will continue to increase with the discontinuity propagation. More elements and nodes are progressively added. The approach was used for a considerable time to analyse discontinuities [33].
- Using a smeared representation of the discontinuity passing through the element. This approach is numerically more efficient than the previous one, as there are no new nodes or elements added. However, there will be some information loss related to the distribution and width of the discontinuity [34].
- Use of relatively new approaches to define the discontinuity such as the extended finite element method [35]. Their applicability to the current issue is open to future research.

Element "S3" was used in the current analysis due to its efficiency as a RF element. But more importantly, to the way used to calculate curvature. To use element "S3" in the current elastic

perfectly-plastic analysis, it has to be modified to allow internal yield lines to pass through the element. This new feature is added by revising the relationship between the bending and the rigid rotation angles (6) and the relationship between the rigid rotation angles and the out-of-plane displacements (7) for elements with internal yield line. Details of the modifications introduced in this research to element "S3" are as following:

2.2.2. Adding yield lines to element "S3"

The main concepts behind the current research are the following:

a- Allowing yield lines to pass through the element.
b- Incorporating plastic rotation at the element sides with the rigid rotation angles.

To add feature (a) above, a method related to the hand calculations of yield line analysis is used. The energy dissipated by a yield line due to a virtual rotation can be calculated by projecting the yield line into other directions, usually the global horizontal and vertical axes in the slab plane [3, 5]. As for feature (b) above, the particular nature of element "S3", especially, the way curvature is calculated, makes this possible.

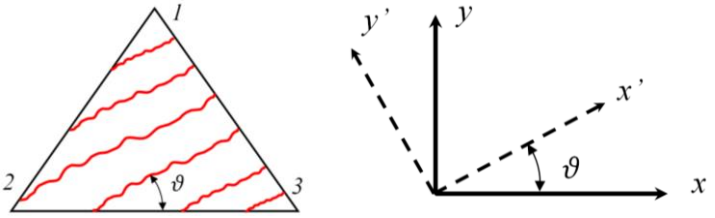

Fig. 5. Yield line local coordinate system (x', y') and relation to edge 2-3

For the current research, the effects of a yield line in reducing stiffness are transformed to each of the three sides of the element using tensor transformation as described below.

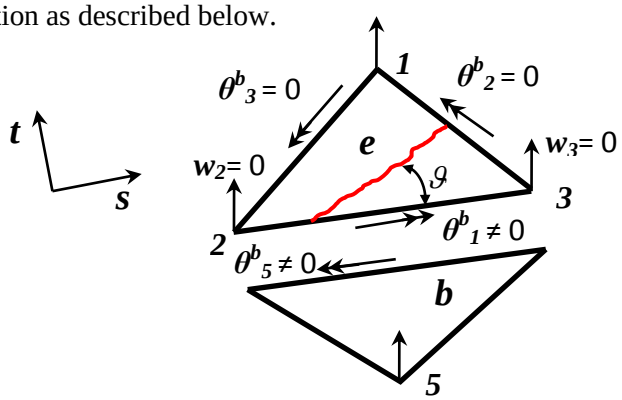

Fig. 6. Imposed boundary conditions to find stiffness at edge 2-3

The effects of an internal yield line inclined at angle (ϑ) relative to side (*2-3*) of the triangle, Fig. 5, is used here as an example of the procedure that is applicable to the three sides of the element. This side is facing node (*1*) of element (*e*). For that, this side is called edge (*1*) of element (*e*). The presence of the internal yield line will reduce the tangent stiffness in the direction normal to the yield line to zero. This is equivalent to stating that the tangent bending curvature across the yield line is zero.

The general two-dimensional transformation matrix for a general tensor [*] from coordinate system (*x',y'*) to (*x,y*) can be expressed as [36]:

$$[*]_{x,y} = [T]^{-1}[*]_{x',y'} \tag{11}$$

$$[T]^{-1} = \begin{bmatrix} cos^2\vartheta & sin^2\vartheta & -2sin\vartheta\, cos\vartheta \\ sin^2\vartheta & cos^2\vartheta & 2sin\vartheta\, cos\vartheta \\ sin\vartheta\, cos\vartheta & -sin\vartheta\, cos\vartheta & cos^2\vartheta - sin^2\vartheta \end{bmatrix} \tag{12}$$

For isotropic slabs, the presence of a yield line along the local (*x'*) axis denotes a normal principal stress direction. As such, the (*x', y'*) coordinate system of Fig. (5) is coincident with the principal directions. Hence the local (*x'*) axis coincides with the yield line direction that is inclined at angle (ϑ) relative to edge (*1*), Fig. 6.

After deformation of element (*e*) and the adjacent element along edge (*1*), Figs. 4 and 6, the following relation can be established [32]:

$$\theta_1^b = \theta_1 - \theta_1^r;\ \theta_5^b = \theta_5 - \theta_5^r\ ;\ \theta_5 = -\theta_1 \tag{13}$$

If the stiffness of the two elements on the sides of the interface is (K_1) and (K_5), then the interface equilibrium is:

$$-K_1\theta_1^b = -K_5\theta_5^b \tag{14}$$

$$\left(1 + \frac{K_1}{K_5}\right)\theta_1^b = -(\theta_1^r + \theta_5^r)\ ;\ \text{or}\ \theta_1^b = -\frac{\theta_1^r + \theta_5^r}{c}\ , where\ c = 1 + \frac{K_1}{K_5} \tag{15}$$

If the two elements have the same stiffness, then (*c = 2*). Otherwise it will differ. The method adopted in Ref. [32] to determine the relative stiffness of the two elements sharing the same interface was based on considering the main element (*e*) with zero out-of-plane displacements at the three nodes and zero rotation at the three sides except for the side under consideration. So, to obtain K_1 the following boundary conditions are used: $w_1, w_2, w_3 = 0, \theta_4 = 0, \theta_6 = 0, \theta_5 \neq 0$, Fig. 6.

The virtual work of element (*e*) due the rotation of interface moment $\bar{M}_5$ by a virtual rotation of $\delta\theta_1^b$ can be expressed as:

$$\delta\theta_1^b \bar{M}_5 = \int \lfloor \delta\varepsilon \rfloor \{\sigma\} dV = \int \lfloor \delta K \rfloor z[D] z\{K\} dV = A\lfloor \delta K \rfloor [\bar{D}]\{K\} = A\lfloor \delta\kappa \rfloor [R_e]^T [\bar{D}][R_e]\{\kappa\} \tag{16}$$

$$\text{where } [\bar{D}] = \int D\, z^2 dz = \frac{Et^3}{12(1-v^2)} \begin{bmatrix} 1 & v & 0 \\ v & 1 & 0 \\ 0 & 0 & \frac{1-v}{2} \end{bmatrix} \tag{17}$$

$$\{\kappa\} = [H_e] \begin{Bmatrix} \theta_1^b \\ \theta_2^b \\ \theta_3^b \end{Bmatrix} = [H_e] \begin{Bmatrix} \theta_1^b \\ 0 \\ 0 \end{Bmatrix} = \begin{bmatrix} 2/h_1 & 0 & 0 \\ 0 & 2/h_2 & 0 \\ 0 & 0 & 2/h_3 \end{bmatrix} \begin{Bmatrix} \theta_1^b \\ 0 \\ 0 \end{Bmatrix} = \theta_1^b \begin{Bmatrix} 2/h_1 \\ 0 \\ 0 \end{Bmatrix} \tag{18}$$

where h_1, h_2 and h_3 are as shown in Fig. 4

$$\lfloor \delta\kappa \rfloor = \lfloor \delta\theta_1^b \quad 0 \quad 0 \rfloor [H_e]^T = \lfloor \delta\theta_1^b \quad 0 \quad 0 \rfloor \begin{bmatrix} 2/h_1 & 0 & 0 \\ 0 & 2/h_2 & 0 \\ 0 & 0 & 2/h_3 \end{bmatrix} = \delta\theta_1^b \lfloor 2/h_1 \quad 0 \quad 0 \rfloor \tag{19}$$

$$[R_e] = \begin{bmatrix} c_1^2 & c_2^2 & c_3^2 \\ s_1^2 & s_2^2 & s_3^2 \\ 2c_1s_1 & 2c_2s_2 & 2c_3s_3 \end{bmatrix} \tag{20}$$

where: $c_1 = \frac{y_3 - y_2}{L_1};\ s_1 = -\frac{x_3 - x_2}{L_1};\ c_2 = \frac{y_1 - y_3}{L_2};\ s_2 = -\frac{x_1 - x_3}{L_2};\ c_3 = \frac{y_2 - y_1}{L_3};\ s_3 = -\frac{x_2 - x_1}{L_3}$

x_i, y_i: *x* and *y* coordinates of node *i*, Figs. 5 and 6

L_i: length of element side facing node *i*, Figs. 5 and 6

However, the presence of the yield line affects the curvature inside the element as well as the material stress-strain relation. In this case, local matrix $[\bar{D}']$ degenerates to:

$$[\bar{D}'] = \frac{Et^3}{12} \begin{bmatrix} 0 & 0 & 0 \\ 0 & 1 & 0 \\ 0 & 0 & \mu \end{bmatrix} \tag{21}$$

where μ is the poisons ratio after the establishment of the internal yield zone.

Considering the simple case of $\mu = 0$, the transformation of matrix $[\overline{\mathrm{D}}']$ from the yield line local axes (x', y') to the global (x, y) axes is as following:

$$[\overline{\mathrm{D}}] = [\mathrm{T}]^{-1}\left[\overline{\mathrm{D}}'\right]([\mathrm{T}]^{-1})^{\mathrm{T}} = \frac{Et^3}{12}\begin{bmatrix} sin^4\vartheta & sin^2\vartheta\, cos^2\vartheta & -sin^3\vartheta\, cos\vartheta \\ sin^2\vartheta\, cos^2\vartheta & cos^4\vartheta & -cos^3\vartheta\, sin\vartheta \\ -sin^3\vartheta\, cos\vartheta & -cos^3\vartheta\, sin\vartheta & sin^2\vartheta\, cos^2\vartheta \end{bmatrix} \quad (22)$$

Substituting Eqs. (18, 19, 20 and 22) into Eq. (16) results in:

$$\delta\theta_1^b \overline{M}_5 = A\lfloor\delta\kappa\rfloor[\mathrm{R_e}]^{\mathrm{T}}[\overline{\mathrm{D}}][\mathrm{R_e}]\{\kappa\} = A\left\lfloor\delta\theta^b\right\rfloor[H_e]^T[\mathrm{R_e}]^{\mathrm{T}}[\overline{\mathrm{D}}][\mathrm{R_e}][H_e]\{\theta^b\} \quad (23)$$

Hence the stiffness of edge (*1*) of element (e) with the presence of a yield line, $K_{1,YL}$, is:

$$K_{1,YL} = \frac{\bar{M}_5}{\theta_1^b} = A\begin{bmatrix}\frac{2}{h_1} & 0 & 0\end{bmatrix}[\mathrm{P_e}]\begin{Bmatrix}\frac{2}{h_1}\\0\\0\end{Bmatrix} = \frac{4A}{h_1^2}\, p_{e,11} = \frac{2L_1}{h_1}\, p_{e,11} \quad (24)$$

where:

$[\mathrm{P_e}] = [\mathrm{R_e}]^{\mathrm{T}}[\overline{\mathrm{D}}][\mathrm{R_e}]$ and $p_{e,11}$ is element (*1,1*) of matrix $[\mathrm{P_e}]$

A similar expression can be obtained for element (*b*), Figs. (4 and 6):

$$K_5 = \frac{2L_1}{h_5}\, p_{b,33} \quad (25)$$

The stiffness ratio of element (*e*) to that of element (*b*) can be expressed as:

$$\frac{K_{1,YL}}{K_5} = \frac{p_{e,11}}{p_{b,33}}\frac{h_5}{h_1} = \eta_{5,YL}\,\frac{h_5}{h_1} \quad (26)$$

With that, a relationship between rigid and bending angles can be established using Eq. (15).The value of η_5 is (*1.0*) for elastic isotropic material of the same thickness. However, the presence of a yield line will change this value depending on its inclination relative to the element edge. The closed form expression for $K_{1,YL}$, Eq. (24), is quite elaborate. However, it can be simplified as described below.

The boundary conditions and side loads imposed on the element cause bending in one direction around element side *2-3*. As the required stiffness is coincident with this direction, a new element local coordinate system (*s*, *t*) can be defined, Fig. 6, such that local axis (*s*) is parallel to side (*2-3*). If the yield line is inclined at an angle (ϑ) relative to the considered element side rather than the global axes as shown in Fig. (6), then, the quantities c_1 and s_1 can be expressed in the element local coordinate system as following:

$$c_1 = \left(\frac{y_3-y_2}{L_1}\right)_{global} = \left(\frac{t_3-t_2}{L_1}\right)_{local} = 0;\ s_1 = -\left(\frac{x_3-x_2}{L_1}\right)_{global} = -\left(\frac{s_3-s_2}{L_1}\right)_{local} = -1 \quad (27)$$

Substituting these values into Eq. (25) results in the following expression for K_1 when μ is assumed to be zero:

$$K_{1,YL} = \left(\frac{2L_1}{h_1}\right)\left(\frac{Et^3}{12}\right)sin^4\vartheta \quad (28)$$

For the general case of $\mu \neq 0$, the following expression is obtained:

$$K_{1,YL} = \left(\frac{2L_1}{h_1}\right)\left(\frac{Et^3}{12}\right)(sin^4\vartheta + 4\,\mu\, sin^2\vartheta\, cos^2\vartheta) \quad (29)$$

When this result is compared with the normal case with no yield lines of $K_1 = \left(\frac{2L_1}{h_1}\right)\left[\frac{Et^3}{12(1-v^2)}\right]$, it becomes clear that the effect of the yield line inclined at an angle (ϑ) with the element side on the stiffness across that side is a reduction of magnitude $(sin^4\vartheta + 4\,\mu\, sin^2\vartheta\, cos^2\vartheta)\,(1-v^2)$.

As a result, (η_5) is changed to ($\eta_{5,YL}$) by multiplying with $(sin^4\vartheta + 4\,\mu\, sin^2\vartheta\, cos^2\vartheta)\,(1-v^2)$. Similar expressions are obtained for (η_4 and (η_6) for the other two sides of the element. These

changes will affect matrix $[H_v]$ used to relate the bending to rigid angles, Eq. (6). In the present analysis the value of μ was taken as zero.

The resulting effect of the yield lines on the finite element is similar in nature to the smeared representation of discontinuity in a plane stress finite element.

2.2.3. Yield Condition of isotropic slab

A slab with the same moment resistance in two orthogonal directions is an isotropic slab. The yield condition of such a slab is called the "square yield condition" by Johansen [3]. According to this condition, the slab moment resistance is the same at any direction; hence it is an isotropic quantity. The yield condition is satisfied when the principal moment(s) attain the moment resistance. The direction of the yield line coincides with the principal moment direction.

2.2.4. Material constitutive relationship

In this research, material is assumed to be elastic perfectly-plastic, leading to an elastic perfectly-plastic moment curvature relation. This material model allows elastic deformations to be calculated. It also allows efficient solution of the non-linear equilibrium equation as described in section 2.4.

2.2.5. Load factor required to satisfy the yield condition

At the start of a new load increment (i) the total moments of an element resulting from previous loads can be represented by $\boldsymbol{M^{i-1}} = (M_x^{i-1}, M_y^{i-1}, M_{xy}^{i-1})$. When the load is applied at increment (i) and structure is analysed, the resulting increment moments of the element are, $\Delta\boldsymbol{M}^i = (\Delta M_x^i, \Delta M_y^i, \Delta M_{xy}^i)$. The total moment is the summation of the previous total moments and the incremental moments multiplied by the load factor (λ) such that $\boldsymbol{tM}^i = \boldsymbol{M^{i-1}} + \lambda\Delta\boldsymbol{M}^i$. The load factor is obtained from equating the total moment to the moment capacity.

2.2.6. Load factor required to create a second yield line in an element with a single yield line

If an element has a single yield line, then there is a possibility that a second one can develop. The two yield lines are orthogonal to each other as they follow the principal directions. The load factor required to cause the second yield line is obtained by comparing the total moment and moment capacity at a direction normal to the first yield line.

2.3. Method limitations

Currently, the method can only consider flexural yielding. No shear or axial effects are considered. It is also limited to small displacement analysis with no geometric non-linearity considered.

2.4. Implementation in finite element analysis

The nature of yield line analysis, being based on rigid perfectly-plastic behaviour, can be used to simplify the non-linear analysis to a large extent. In this analysis the material is assumed to be elastic perfectly-plastic. As a result, once a yield line is formed, the moment across it remains constant. There are no residual or unbalanced forces generated due to curvature increase. This assumption is valid for under-reinforced slabs [37]. Hence it is applicable to most designs.

In the current research, the analysis starts by assembling the stiffness matrix of the structure, applying the boundary conditions and loads. The system is solved and element principal moments are checked against their yield moments. The loads and results are scaled so that the element(s) that are closest to their yield moment attain that value. Yield lines are created at these elements in the direction of principal moment. Element stiffness in the direction perpendicular to the yield line direction(s) is

reduced to a small value rather than zero to avert possible numerical instability. By then, the first load increment is complete. The same steps are repeated for the next load increment.

The residual forces after each load increment are zero. This feature negates the need for iterations to satisfy equilibrium, as the system will be in equilibrium after each load increment. As a result, the solution time required to solve the structure is substantially reduced.

The convergence criteria currently used is related to the deflection of a selected point. Two ratios are compared. The first is the maximum displacement ratio defined as the maximum ratio, of incremental deflection at the node to the total deflection at that node. The second ratio is the load ratio which is the incremental load ratio. The solution stops when the displacement ratio is (α) times more than the load ratio. In addition, the results can be shown at any stage of loading. The user has full control over the computer program and can stop the analysis at any desired stage.

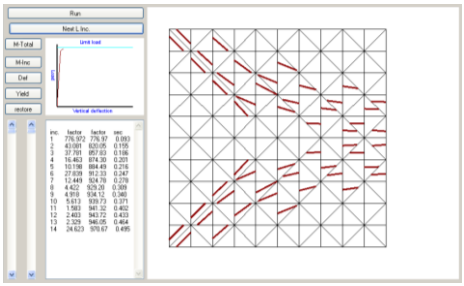

Fig. 7. Computer program user interface

The procedure detailed above was implemented in a computer program code that can run on ordinary office computers. Graphical user interface was developed to simplify presenting the analysis results. Unreformed geometry, deflected shape, and principal bending moment magnitudes and directions, as well as the location and direction of yield lines can be presented at any time during any analysis stage. To help identifying critical load, a load-deflection curve of any selected point is also shown. The program is interactive with the user and has the interface shown in Fig. 7.

3. Examples

To demonstrate the accuracy and performance of the proposed method, seven examples were solved. Four are presented in detail, while the other three are presented in a compact table format due to space limits. All results were compared with yield line analysis results and these obtained from ANSYS-10 non-linear finite element analysis. The computer program was run on machine with a 2.8 GHz Intel Pentium D915 processor. All execution times stated in the following paragraphs were measured on this machine.

3.1. Example-1: simply supported square plate with one free side subjected to uniform load

The geometry, dimensions and boundary conditions of the slab are shown in Fig. 8 (a). This slab was previously solved by Wüst and Wagner [22] using their method for systematically finding all possible yield patterns. For a 1.0 kNm/m plastic moment capacity, an ultimate load of 14.14 kN/m^2 was reported. This result was also verified using a non-linear finite element analysis, Fig. 8 (b) [22].

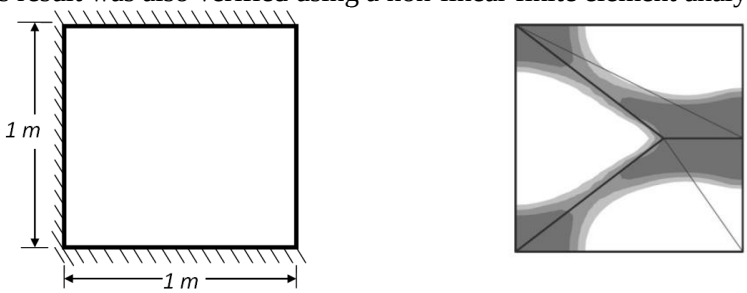

(a) Geometry and boundary conditions (b) Finite element yield zones [22]

Fig. 8. Geometry, boundary conditions and previous results of example-1

A load of 1.0 kN/m^2 was applied in the current analysis; hence a load factor (LF) of 14.14 corresponds to the above result. This is the value used in the following comparisons. The plate was initially modelled using the 10x10 grid mesh shown in Fig. 9. The resulting load factor, progress of yield lines and deflections are also shown in the same Figure. The load factor obtained from the present analysis of 14.08 is close to the previously reported value of 14.14 with a difference of less than 0.5% between the two.

A sensitivity study was conducted to find the effect of mesh density on the results. The following mesh grids were studied: 6x6, 20x20 and 50x50 as shown in Fig. 10. Load factors and yield pattern are shown in Fig. 10 for the three meshes.

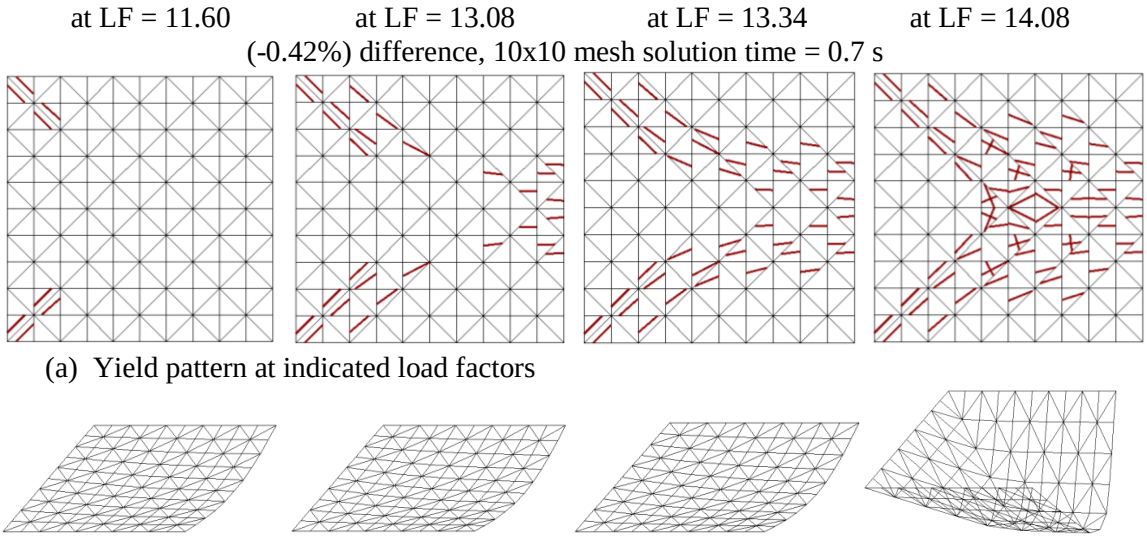

(a) Yield pattern at indicated load factors

(b) Deflected shapes at indicated load factors

Fig. 9. Results of simply supported square plate with one free side, subjected to uniform load

All load factors were in close agreement with both the results obtained from the 10x10 mesh grid and the value reported in Ref. [22]. Maximum difference was +0.57% resulting from the coarse mesh. It is observed from these results that reasonable accuracy was obtained from the three meshes and that accuracy is not very sensitive to mesh refinement. The execution times for the 6x6, 10x10, 20x20 and 50x50 examples were 0.2, 0.7, 7.7 and 177.9 seconds respectively. The yield pattern at failure had the expected arrangement. More refined yield pattern was obtained from the finer meshes. However, the yield pattern resulting from the different meshes have similar overall arrangements.

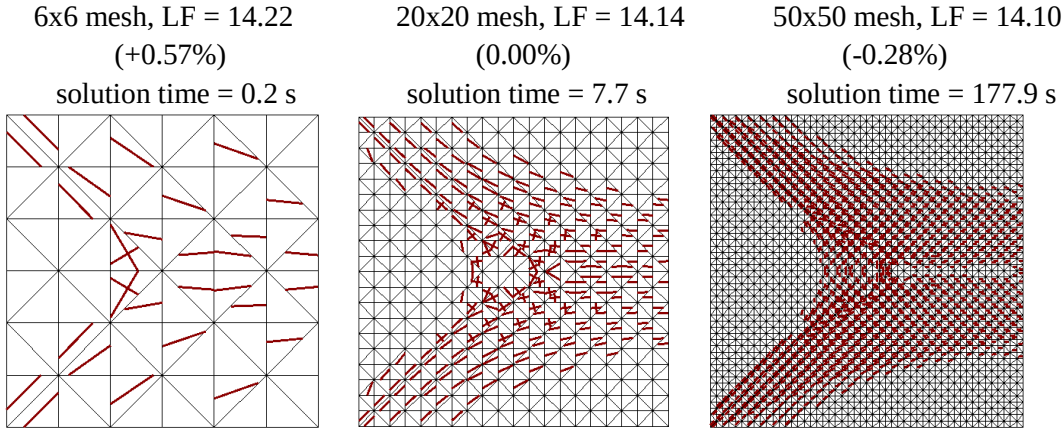

Fig. 10. Sensitivity study Yield pattern of simply supported square plate with one free side

3.2. Example-2: simply supported square plate subjected to central concentrated load

A simply-supported, square plate subjected to central concentrated load was studied next. The yield line failure load for this classic slab example was: $M_F/L^2 = 8.0\ kN/m^2$ [38], where M_F is the slab moment capacity per unit width and L is the slab side length. Hence the load factor of the slab is 8.0. A positive moment capacity of 1.0 kNm/m was used herein. A load factor of 7.99 was obtained from a 10x10 mesh grid. This was within 0.13% of the theoretical value. The yield pattern and final deflected shape are shown in Fig. 11. Solution time was 0.29 s. Yielding, Fig. 11 (a), started at the centre of the plate at around 56% of the failure load. Failure was due to yielding along the full length of the diagonals and tangential yielding of the central elements. The central elements developed yielding in two directions which resulted in the final failure.

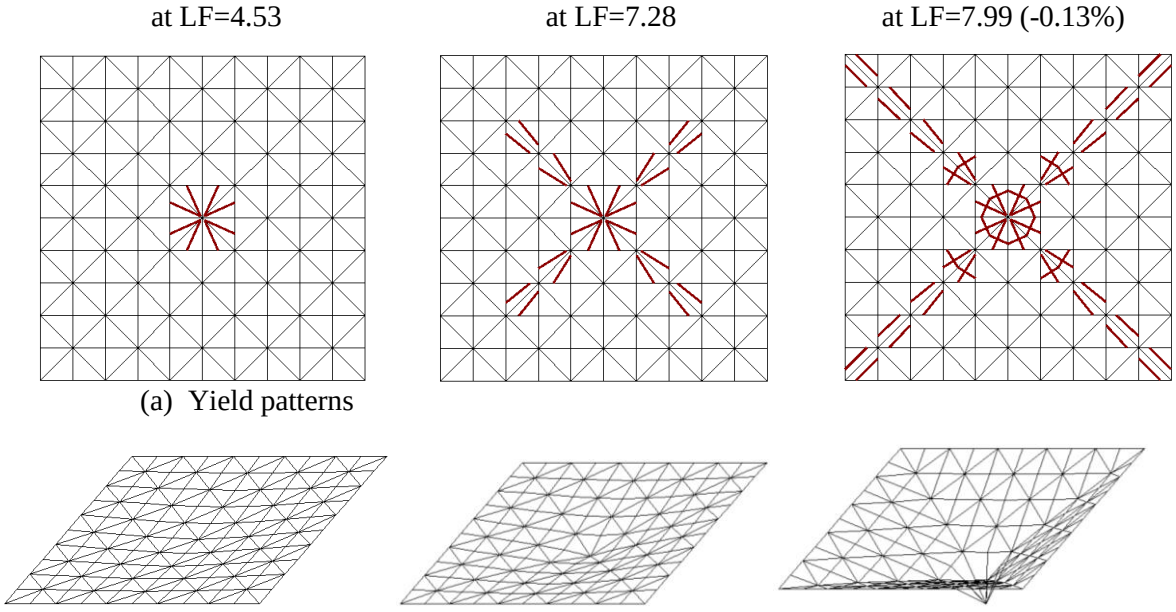

Fig. 11. Results of simply supported square plate subjected to uniform load, 10x10 mesh

A sensitivity study was conducted to find the effect of mesh density on the results. The following mesh grids were studied: 4x4 and 20x20. Load factors and final yield patterns are shown in Fig. 12. The load factor obtained from the 4x4 and 20x20 mesh grids were 8.01 and 8.00, respectively. All results were within 0.13% of the classical solution. These results show good accuracy from the different meshes and low sensitivity to mesh refinement. The yield pattern resulting from the current analysis was as expected. This was the case for all the meshes, even the coarse 4x4 mesh. Some of the elements had two orthogonal yield lines. These elements were located near the central part of the slab. Symmetry of the yield pattern is obvious in Fig. 12. The execution times for the 4x4, 10x10 and 20x20 examples were 0.09, 0.29 and 2.65 seconds, respectively.

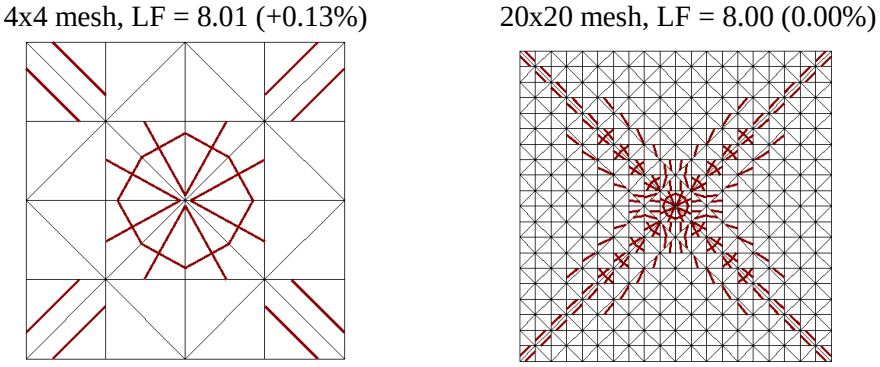

Fig. 12. Yield pattern of simply supported square plate subjected to concentrated load

To verify the results, the same example was analysed with ANSYS. The model was made from a 40x40 mesh made from ANSYS shell 93 element. A von Mises non-linear material model was used. The non-linear analysis could define a collapse load corresponding to a load factor of 6.9. The analysis time was 113 seconds. This result is 13.75% less the yield line results of Ref. [38] and to the current results. Possible reasons for the difference are the distinct yield criteria and element types. The deflected shape and deflected contours are shown in Fig. 13.

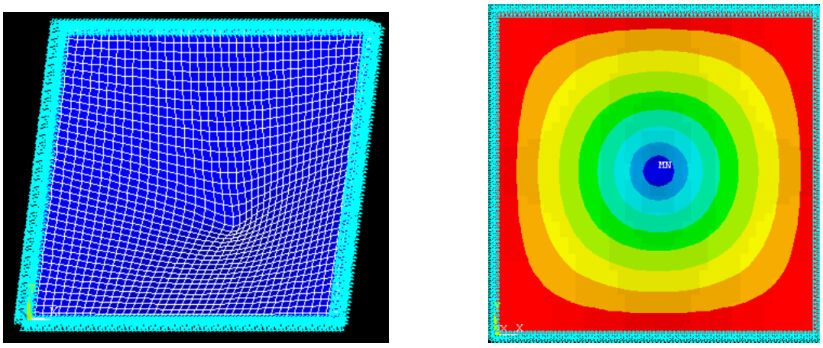

Fig. 13. Deflected shape and contours of Example-2-ANSYS analysis

Behaviour similar to that observed in the previous example was repeated here. Reasonably accurate results were obtained from different meshes, irrespective of mesh fineness.

3.3. Example-3: fixed square plate subjected to uniform load

A fixed square plate subjected to a uniform load was studied in this example. This slab was previously studies by many researchers as reported in Table 1. As stated in section 1, Burgoyne and Smith [24] predicted a load factor of 41.19. In the current analysis, the reference load factor used for the following comparisons is the 42.85 shown in Table 1 [24].

A 10x10 finite element mesh was used to analyse the slab. The progress of yielding and distribution of principal bending moments are shown in Fig. 14.

Method	QL^2/m_p	Factor
Linear elastic finite element	6·84	0·160
Lower bound with simple diagonal strips	16	0·373
Lower bound with optimised diagonal strips	25·13	0·586
Lower bound with two strips parallel to sides	32	0·747
Lower bound with four strips	41·19	0·961
Fox's exact solution [10]	42·85	1
Best yield line: Mansfield[19] and Morley[20]	42·88	1·001
COBRAS yield line	43·99	1·026
Fully plastic finite element	47·63	1·112
Classic yield line analysis	48	1·120

Table 1. Load factor for fixed square plate subjected to uniform load using various analysis methods (reproduced from [24])

The load factor of 42.57 was obtained from a 10x10 mesh grid with -0.65% difference from the reference value. The analysis time was 2.4 s.

As shown in Fig. 14, yielding started at the mid-length of the fixed four sides. The yield lines resulting from negative moments were nearly parallel to the sides. Yielding due to negative moment continued on the fixed sides of the slab until it covered the whole perimeter of the. The yield line

directions changed near the four corners to create a more curved yielded layout. Yield resulting from a positive moment started at the diagonals and extended rapidly towards the plate centre and the four corners. They intersected at the slab centre where elements with two yield directions were created.

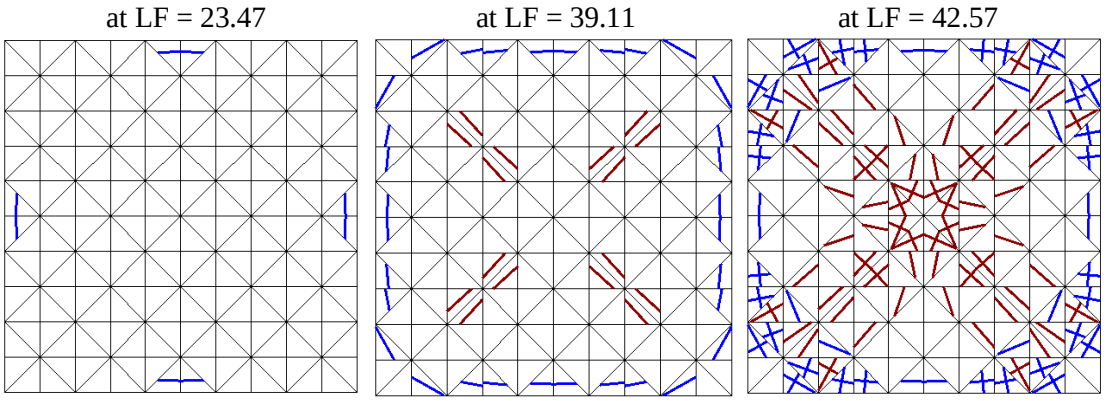

Yield pattern (red: +ve, blue: -ve)

Fig. 14. Yield pattern of fixed square plate with subjected to uniform load, 10x10 mesh

A sensitivity study was conducted to determine the effect of mesh density on the results. The following mesh grids were studied: 4x4, 20x20 and 30x30. Results from these meshes are presented in Table 2 and Fig. 15. The load factors obtained from all the studied meshes were consistently close to the reference solution with only a small change resulting from mesh refinement. This is even true for the unusually coarse 4x4 mesh. More accurate results were obtained with finer meshes at the cost of more solution time. However, even for the densest 30x30 mesh, the solution time was 44.5 s. In an engineering design office environment this time is not excessive for this type of analysis.

Mesh	Load factor	Difference from reference solution	Solution time (s)
4x4	43.66	+1.9%	1.5
10x10	42.57	-0.66%	2.4
20x20	42.55	-0.70%	11.8
30x30	42.76	-0.21%	44.5

Table 2. Sensitivity study of fixed square plate subjected to uniform load

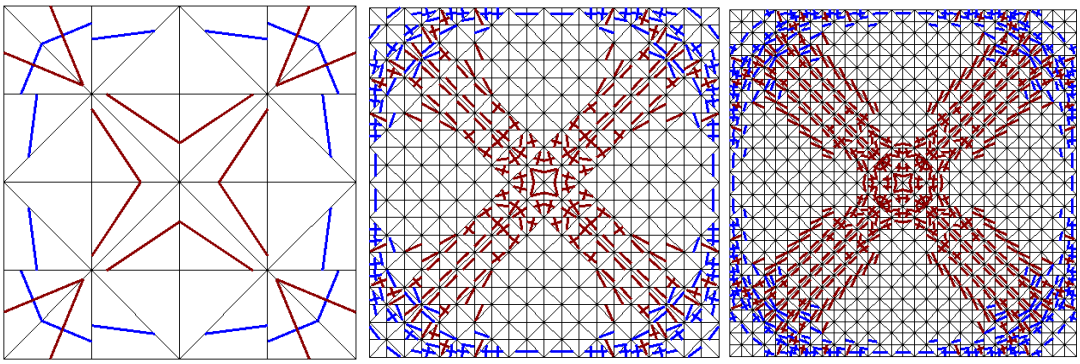

4x4 mesh 20x20 mesh 30x30 mesh

Fig. 15. Sensitivity study results of fixed square plate subjected to uniform load, (red:+ve, blue:-ve)

To verify the results, the same example was analysed with ANSYS using the same element type and material model as used in the previous example. The model was made from a 20x20 mesh for ¼ model. The non-linear analysis could define a collapse load corresponding to a load factor of 40.73.

The analysis time was 45 second. This result was 4.95% less than the reference value of 42.85. Behaviour similar to that observed in the previous examples was repeated here with reasonably accurate results obtained from different meshes, irrespective of mesh fineness.

Example-4: simply supported rectangular flat slab subjected to uniform load

A large reinforced concrete flat slab with 3x3 bays and a grid of 8.0m in both directions shown in Fig. 16 was analysed to show the capability of the proposed method in analysing practical size slabs. This size of slabs is not unusual in normal design office work. It is usual to analyse such regular slabs using Code methods or using elastic finite element analysis. In this example, a load of 1 kN/m^2 was applied. The plastic moment capacity was 200 kNm/m for both sagging and hogging moments. The analysis was conducted using the following three meshes: 14x14, 28x28 and 42x42. All supports were assumed to be pinned. No use of symmetry was made in order to verify the symmetry of results and to demonstrate the capability of the new method in cases of unsymmetrical slabs. It was assumed that there was sufficient shear resistance to guarantee a flexural failure. It was also assumed that the ultimate strain limits of neither steel nor concrete were exceeded.

The progress of yielding with increased load is shown in the 28x28 mesh model shown in Fig. 17. At around 41% of the failure load, extensive yielding over the internal columns was observed (Fig. 17). This is expected behaviour of flat slabs, where concrete cracking and possible yielding of reinforcement appear at service load levels. The total solution time was 52.5 seconds.

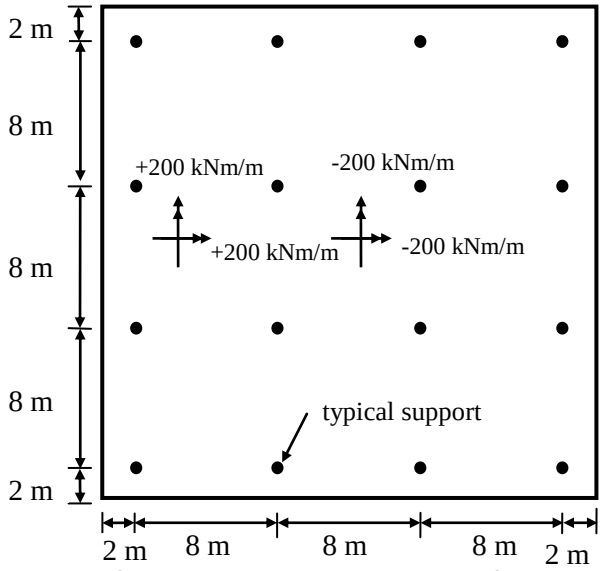

Fig. 16. Layout of large flat slab example

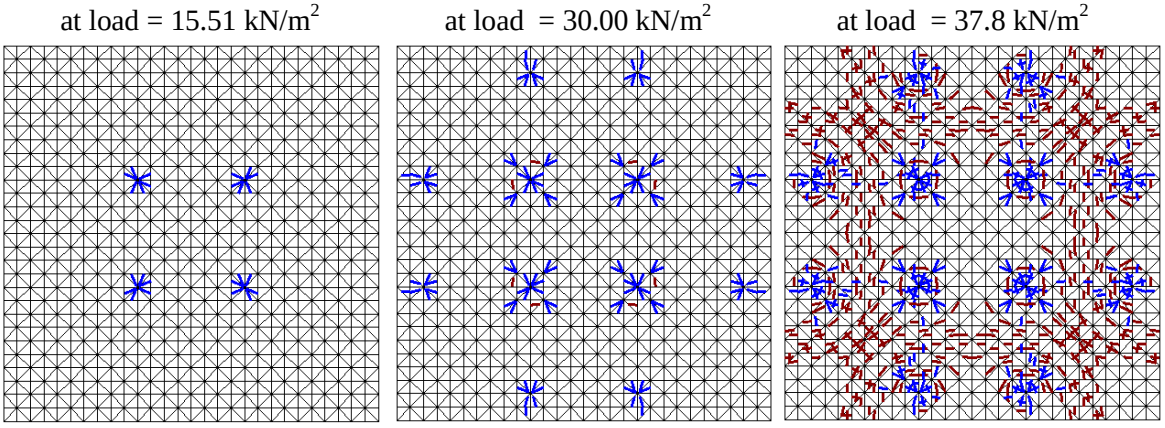

Fig. 17. Yield pattern of large isotropic flat slab example, 28x28 mesh (red: +ve, blue: -ve)

To verify the results, the same example was analysed with ANSYS using the same element type and material model as used in the previous examples. The model was made from a 28x28 mesh for ¼ of the slab. The non-linear analysis could define a collapse load corresponding to a load factor of 33.5. The analysis time was 46 second. This result was 11.38%-16.04% less than the current results of 37. 8-39.9. Possible reasons for the difference are the distinct yield criteria and element types.

A sensitivity analysis was made to study the effect of mesh refinement on results. Three meshes were studied. These were 14x14, 28x28, and 42x42 meshes. The results are shown in Fig. 18. The load factor obtained from the three meshes was 39.9, 37.8 and 37.8 signifying a failure load of 39.9 kN/m2, 37.8 kN/m2 and 37.8 kN/m2 for the 14x14, 28x28 and 42x42 meshes respectively. These results differed by 5.5% between the least and most dense meshes. The solution time for the three meshes was 3.6 second, 52.5 second and 262.9 seconds. The yield pattern resulting from the three meshes showed the expected behaviour with most of the yielding concentrated around the columns and the external spans. The deflected shape of the slab is shown in Fig. 18 (b). The early yielding around the internal columns was in the form of an inverted cone. At failure, the remaining central part of the slab moved down as a rigid body.

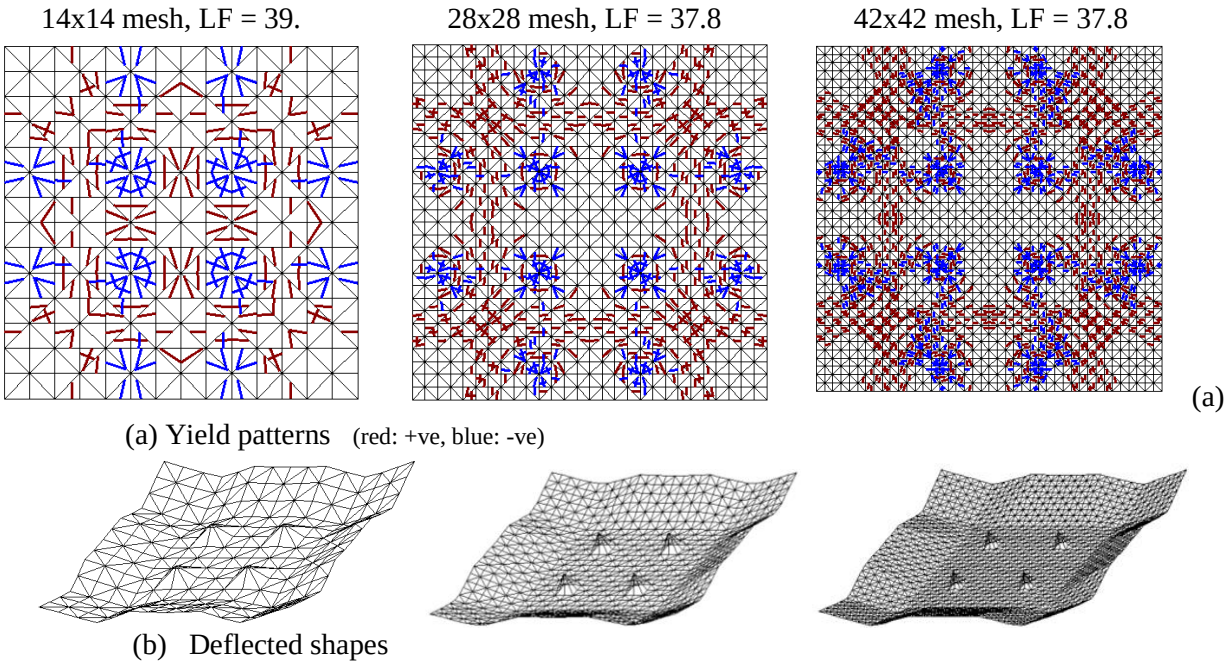

Fig. 18. Results of large flat slab example

3.4. Examples-5 to 7

Due to space limitations, the following examples are presented below in a table format. As shown in Table 3, all the results obtained from the current method are reasonably accurate when compared to both yield analysis results and those obtained from the finite element non-linear analysis using ANSYS.

Example No.	Description	Geometry	Reference result	ANSYS result	Current result
5	Two way simply supported square slab subjected to uniform load	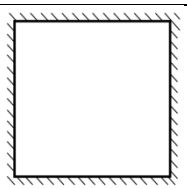	24 [38] (100.0%)	23.1 20x20 mesh (96.2%)	24 10x10 mesh (100.0%)
6	One way simply supported square slab subjected to uniform load	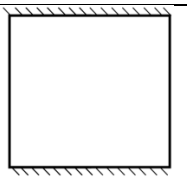	8 [5] (100%)	8 20x20 mesh (100.0%)	8 10x10 mesh (100.0%)
7	Propped cantilever slab subjected to uniform load	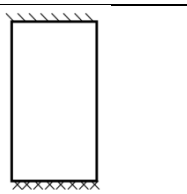	14.57 [40] (100%)	15.5 20x40 mesh (106.4%)	14.5 10x20 mesh (99.5%)

Table 3. Results of examples 5-7, values in ( ) are relative to reference solution

4. Conclusions

This paper presents the development, implementation and selective benchmark of a new method to be a practical alternative to current practice yield line analysis, strip method, and non-linear finite element solutions free from the limitations and difficulties encountered when using these methods.

The use of RF plate triangular elements in the non-linear elastic perfectly-plastic analysis of plates is computationally efficient due to their single degree of freedom per node. The ability to define a plastic "yield line" to pass through an element resolves the limitation that "yield lines" can only pass through element boundaries. This feature eliminates the need to revise the finite element mesh using computationally expensive optimization techniques or mesh refinements to satisfy the condition that "yield lines" must pass through element boundaries. By following the spirit of the yield line analysis, the effects of a plastic "yield line" is projected to the element sides and used to calculate the bending curvatures. That was made possible by the way curvature is calculated in element "S3".

By applying the load in increments that cause the generation of new plastic zones, the solution is incremental. Iterations are not required, as the structure is in equilibrium at the start and end of each load increment. No residual or unbalanced forces are generated. This results in a numerically stable and efficient solution.

The new method can predict yield line analysis results accurately and efficiently with the added advantage that it is finite element based. Additionally, the results are not limited to a load factor and a failure pattern, but include deflections, reactions and moments at all nodes and elements. These results are available not only at the failure load but along the full loading history. The accuracy of the method, its efficiency and ability to solve practical sized reinforced concrete slabs are demonstrated in the solved examples. The method is currently applied to isotropic slabs with the aim of extending it to non-isotropic slabs in the future.

References

[1] Ingerslev, A., "Om en elementær beregningsmetode af krydsarmerede plader, in Danish (On a Simple Analysis of Two-Way Slabs)", Ingeniøren, 30, 69, 1921, pp 507-515. (See also:"The Strength of Rectangular Slabs", Struct. Eng., 1, 1, 1923:3-14.)
[2] Johansen, K.W., "Beregning af krydsarmerede jernbetonpladers brudmoment", in Danish. Bygningsstatiske Meddelelser, 3, 1, 1931:1-18.
[3] Johansen, K.W., Brudlinieteorier, Gjellerup, Copenhagen, 1943, 189 pp. (English translation: Yield-Line Theory, Cement and Concrete Association, London, 1962).
[4] Nielsen, M.P., Limit analysis of reinforced concrete slabs, Acta Polytechnica Scandinavica, Civil Engineering and Building Construction Series, 26, 1964.
[5] Jones, L. L. and Wood, R. H. Yield line analysis of slabs. Thames & Hudson, London, 1967.
[6] Packer, J. A. and Morris, L. J., A limit state design method for the tension region of bolted beam-column connections, The Structural Engineer, 1977, 55(10):446-458.
[7] Joints in steel construction, Moment connections, The Steel Construction Institute, 1995.
[8] Steel Design Guide 1: Base plate and anchor rode design, American Institution of Steel Construction, Chicago, Illinois, 2nd edition, 2006.
[9] Sinha, B. P. and Henry, A. W., Johnson, The stability of a five-storey brickwork cross-wall structure following the removal of a section of a main loadbearing wall, The Structural Engineer, 1971, 49(10):467-474.
[10] Haseltine, B. A., West, H. W. H. and Tutt, J. N., Design of walls to resist lateral loads, The Structural Engineer, 1977, 55(10):422-430.
[11] Johnson, D., Collapse analysis of reinforced concrete slabs: Are the up and down roads one and the same? Advances in Engineering Structures, Mechanics & Construction, 2006, 140(8):823-831.
[12] Munro, J. and Da Fonseca, A. M. A., Yield line method by finite elements and linear programming, The Structural Engineer, 1978, 56B(2):37-44.
[13] Dickens, J. G. and Jones, L. L., A general computer program for the yield-line solution of edge supported slabs, Computers & Structures, 1988, 30(3):465-476.
[14] Johnson, D., Mechanism determination by automated yield-line analysis, The Structural Engineer, 1994, 72(19):323-327.
[15] Johnson, D., Yield-line analysis by sequential linear programming, International Journal of Solids and Structures, 1995, 32(10):1395-1404.
[16] Gohnert, M. and Kemp, A. R., Yield-line elements: for elastic bending of plates and slabs, Engineering Structures, 1995, 17(2):87-94.
[17] Gohnert, M., Collapse load analysis of yield-line elements, Engineering Structures, 2000, 22(8):1048-1054.
[18] Middleton, C. R., Concrete bridge assessment: an alternative approach. The Structural Engineer, 1997, 75 (23&24):403-409.
[19] COBRAS v1.7, Cambridge Enterprise Limited, Cambridge, UK.
[20] Thavalingam, A., Jennings, A., McKeown, J. J. and D. Sloan, D., A computerised method for rigid-plastic yield-line analysis of slabs, Computers & Structures, 1998, 68(6):601-612.
[21] Kwan, A. K. H., Dip and strike angles method for yield line analysis of reinforced concrete slabs, Magazine of Concrete Research, 2004, 56(8):487-498.
[22] J. Wüst, W. and Wagner, W., Systematic prediction of yield-line configurations for arbitrary polygonal plates, Engineering Structures, 2008, 30(7):2081-2093.
[23] Hillerborg, A., Strip Method of Design, Spon Press, 1976.
[24] Burgoyne, C. J. and Smith, A. L., Automated lower bound analysis of concrete slabs, Magazine of Concrete Research, 2008, 60(8):609-622.
[25] O'Dwyer, D. W. and O'Brien, E. J., Design and analysis of concrete slabs using a modified strip method, The Structural Engineer, 1998, 76(17):329-333.
[26] Nay, R. A. and Utku, S., An alternative to the finite element method. Variational Methods Engineering, Southampton University Press, 1972, 1:2/62-74.
[27] Hampshire, J., Topping, B. H. V. and Chan, H.C., Three node triangular bending elements with one degree of freedom per node, Engineering Computations, International Journal for Computer Aided Engineering and Software, 1992, 9(1): 49-62.

[28] Phaal, R. and Calladine, C. R., A simple class of finite elements for plate and shell problems I: Elements for beams and thin flat plates, Int. J. Numer. Methods Engrg., 1992, 35(5):955–977.
[29] Morley, L. S. D., The constant-moment plate-bending element. Journal of Strain Analysis, 1971, 6:20-24.
[30] Sabourin, F. and Brunet, M., Analysis of plates and shells with a simplified three node triangular element, Thin-Walled Structures, 1995, 21(3):209–223.
[31] Onãte, E. and Cervera, M., Derivation of thin plate bending elements with one degree of freedom per node: A simple three node triangle, Engrg. Comput., 1993, 10:543–561.
[32] Sabourin, F. and Brunet, M., Detailed formulation of the rotation-free triangular element S3 for general purpose shell analysis, Engineering Computations, 2006, 23(5):469-502.
[33] Ngo, D. and Scordelis, A.C., Finite element analysis of reinforced concrete beams, ACI Journal , 1967, 64:152-163.
[34] Nilson, A. H., Nonlinear analysis of reinforced concrete by the finite element method. ACI Journal, 1968, 65(9):757–766.
[35] Belytschko, T., Song, J-H. , Gracie, R. and Oswald, J., Advances in the extended finite element method (XFEM), 8th. World Congress on Computational Mechanics (WCCM8), June 30 – July 5, 2008 Venice, Italy.
[36] Jones, R., Mechanics of composite materials, 2nd edition, 1999, Taylor & Francis
[37] Nilson, A., Darwin, D. and Dolan, D., Design of concrete structures, 14th edition, 2009, McGraw-Hill.
[38] Nawi, E. G., "Reinforced concrete, a fundamental approach", 6th edition, 2005, Pearson Education Inc.
[39] Thavalingam, A., Jennings, A., Sloan, D., McKeown, J. J., Computer-assisted generation of yield-line patterns for uniformly loaded isotropic slabs using an optimisation strategy. Engineering Structures, 1999, 21(6):488–496
[40] Ramsay, A. C. A., and Johanson, D., Geometric optimization of yield-line patterns using a direct search method, Structural optimization, 1997, 14(2-3):108-115.